

Ultraviolet emission from Sb-doped *p*-type ZnO based heterojunction light-emitting diodes

L. J. Mandalapu, Z. Yang, S. Chu, and J. L. Liu^{a)}

Quantum Structures Laboratory, Department of Electrical Engineering, University of California at Riverside, Riverside, California 92521, USA

(Received 6 October 2007; accepted 3 March 2008; published online 24 March 2008)

Heterojunction light emitting diodes (LEDs) were fabricated by making Au/Ni top Ohmic contacts on Sb-doped *p*-type ZnO film with low specific contact resistivity and Al/Ti back Ohmic contacts on *n*-type Si substrate. Near-band edge and deep-level emissions were observed from the LED devices at both low temperatures and room temperature, which is due to band-to-band and band-to-deep level radiative recombinations in ZnO, respectively. The electroluminescence emissions precisely match those of photoluminescence spectra from Sb-doped *p*-type ZnO, indicating that the ZnO layer acts as the active region for the radiative recombinations of electrons and holes in the diode operation. © 2008 American Institute of Physics. [DOI: 10.1063/1.2901018]

ZnO, a wide-band-gap semiconductor with large exciton binding energy of 60 meV and high radiation hardness is promising for achieving high-efficiency light-emitting and laser diodes.^{1–4} However, the hindrance in achieving high-efficiency ZnO-based optoelectronic devices is the fabrication of reliable and reproducible *p*-type ZnO material. Therefore, optoelectronic devices based on *n*-ZnO have been reported in plenty. Heterojunction diodes based on *n*-ZnO and other *p*-type semiconductors such as *p*-GaN, *p*-AlGaIn, *p*-SrCu₂O₂, and *p*-Si have been realized.^{4,5} In the past couple of years, the number of studies on light-emitting diodes (LEDs) implementing *p*-ZnO showed a steady increase. This is because of more and more availability of *p*-type ZnO material, which is fabricated using acceptor dopants such as As, P, and N (for example Refs. 6–13). However, many of the devices yield deep-level related emissions with none or small UV emissions.^{8–13} Our research group demonstrated *p*-type ZnO fabrication by using Sb as dopant, which introduces a shallow acceptor level of 160 meV above the valence band as a result of the formation of Sb-2V_{Zn} complexes.^{14,15} Furthermore, we fabricated photodetectors with good performance based on Sb-doped *p*-type ZnO films.^{16–18} In this letter, we report near-band edge emissions from Sb-doped *p*-ZnO/*n*-Si heterojunction LEDs.

Thin undoped ZnO film was grown at low temperature on *n*-Si(100) substrate as a buffer layer, followed by Sb-doped ZnO layer at a higher temperature in molecular beam epitaxy system. Details of growth can be found elsewhere.¹⁹ Thermal activation of the Sb dopant was performed *in situ* in vacuum at 800 °C for 30 min. The resultant thicknesses of undoped and Sb-doped ZnO layers are about 50 and 370 nm, respectively. The elemental distribution of Zn, Sb, and Si was obtained by performing secondary ion mass spectroscopy (SIMS) measurements, as shown in Fig. 1. Since SIMS characterization was performed using O beam, O profile in ZnO was not obtained. Zn and Si depth profiles represent the ZnO film grown on Si substrate. Sb profile extends uniformly in the Sb-doped ZnO, while some Sb atoms have diffused into the undoped ZnO layer, as can

be inferred by the slow decrease of Sb profile in the undoped layer. This indicates the possibility of the undoped layer being converted as *p*-type layer or extensive compensation of electrons in the undoped layer. Electrical properties were determined by Hall effect measurements in a van der Pauw configuration. Hole concentration, mobility, and resistivity of $9.6 \times 10^{18} \text{ cm}^{-3}$, $16 \text{ cm}^2 \text{ V}^{-1} \text{ S}^{-1}$, and $0.04 \Omega \text{ cm}$, respectively, were obtained for the ZnO sample.

Heterojunction LEDs were formed by e-beam evaporation of Au/Ni contacts of size $120 \times 180 \mu\text{m}^2$ on Sb-doped ZnO and Al/Ti contacts on the back side of the *n*-Si substrate. The contacts were annealed at 800 °C for 60 s to obtain Ohmic contacts with fairly low specific contact resistivities.¹⁹ The devices were packaged onto TO5 can using conductive epoxy resin. Current-voltage (*I*-*V*) characteristics were measured using Agilent 4155C semiconductor parameter analyzer, and temperature control was achieved by using a Janis cryostat. *I*-*V* characteristics of the *p*-ZnO/*n*-Si heterojunction device are shown in Fig. 2. The semilogarithmic plot of the *I*-*V* characteristics is shown in the inset. The inverted rectification characteristics with higher leakage current at both higher temperatures and higher biases are ob-

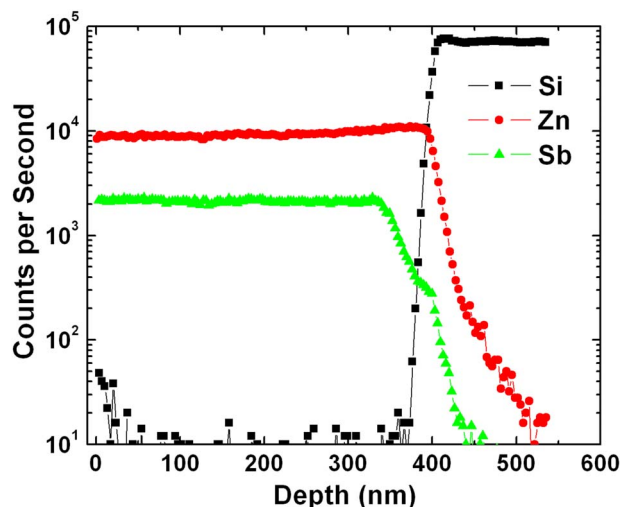


FIG. 1. (Color online) SIMS data of Sb-doped ZnO/ZnO/Si (100) sample. The elemental profiles of Sb dopant, Zn, and Si substrate can be seen.

^{a)} Author to whom correspondence should be addressed. Electronic mail: jianlin@ee.ucr.edu.

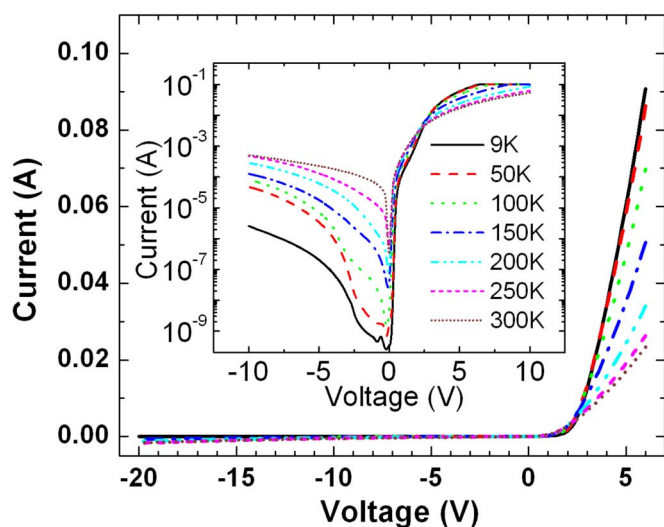


FIG. 2. (Color online) Temperature dependent I - V characteristics of the ZnO-based heterojunction device. Semilog plot of the characteristics is shown as the inset.

served. This result is possibly attributed to the band alignment of wide-band-gap p -ZnO and narrow-band-gap n -Si.¹⁸

Electroluminescence (EL) measurements were performed using an Oriel monochromator and photomultiplier tube. An external power supply was used to inject input current. EL characteristics were obtained by operating the diode in its forward operation region, where positive bias was applied to n -Si. Similar report has been seen on EL from n -ZnO/ p^+ -Si heterojunction diode, where EL is observed in UV region during the positive bias on n -ZnO and is explained by the band alignment.⁵ Figure 3(a) shows the EL spectra obtained at different temperatures for an injection current of 110 mA by setting the monochromator slit size to about 3.3 mm. Four distinct emission peaks around 381 (3.25 eV), 485 (2.5 eV), 612 (2.0 eV), and 671 nm (1.8 eV) can be observed from the spectra at 9 K. The peak around 381 nm is the near-band edge emission. The origin of peak around 485 nm is not very clear although similar emissions were attributed to oxygen vacancies or Zn interstitials in other reports.¹² However, our samples were grown in O rich condition with a lot of Zn vacancies because of which we possibly cannot do a similar assignment. The 612 and 671 nm emissions are believed to be due to intrinsic defects. A small peak around 396 nm (3.13 eV) is also seen in the UV region at 9 K, which is related to Zn vacancies. Figure 3(b) shows the spectra focusing on the UV region only. With increasing temperature, both the small UV peak and the near-band edge emission redshift and appear as a single peak at higher temperatures. The redshift of the UV peak consisting of near-band edge emission and electron-to-acceptor Zn vacancy emission from 381 to about 409 nm for the temperature ranging from 9 to 300 K is due to the temperature induced band gap variations. The intensity of emissions drops throughout the spectra with increasing temperature, which is typical due to the increase in nonradiative recombinations at higher temperatures. The intensity of UV peaks is low compared with deep-level emissions probably due to low radiative efficiency and self-absorption effect induced by deep levels.²⁰

Room-temperature EL at various injection currents is shown in Fig. 4. Although emission from the device could be

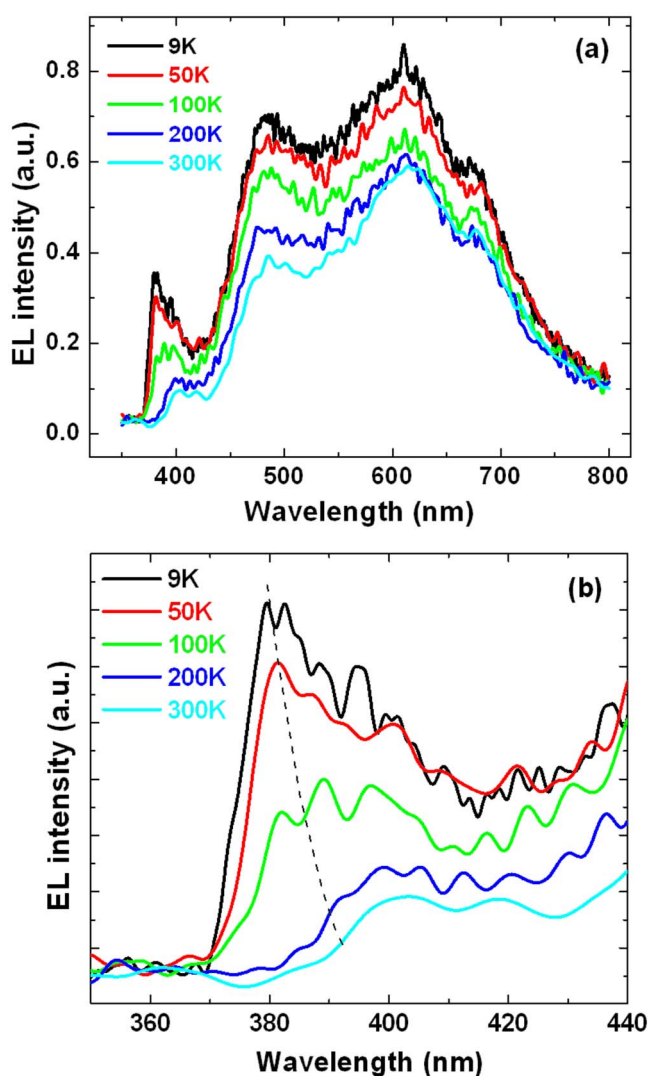


FIG. 3. (Color online) (a) Temperature dependent EL spectra obtained at an injection current of 110 mA. EL from LED is obtained at 9, 50, 100, 200, and 300 K and (b) temperature dependent EL spectra in the UV region only. The dotted line indicates the trend of the redshift of the near-band edge emission from 381 nm at 9 K to about 393 nm at 300 K due to temperature induced band gap variations. The near-band edge emission becomes very weak at 300 K and merges with the UV peak originated from the radiative recombination between conduction band and the Zn vacancy acceptor level. This peak also redshifts from 396 nm at 9 K to 409 nm at 300 K due to the similar temperature induced effect.

observed for injection currents of about 40 mA, higher input currents were used for obtaining stronger UV emissions and clearer spectra. The intensity of the UV emission increases with the increase of injection current. Nevertheless, the deep-level emissions dominate the whole spectra at different injection currents.

To confirm the origin of these EL emissions, photoluminescence (PL) measurements were carried out on the as-grown sample. The excitation source for PL measurements was a 325 nm He-Cd laser. The PL spectra obtained at 9 and 300 K are shown in Fig. 5. The PL spectra in the visible wavelength were collected by using a smaller monochromator slit size of 1 mm instead of 3.3 mm that was used for the UV region and are shown with a small break in the graph. So, effectively, the intensity of PL emissions ratio in visible to UV region is also highly similar to EL emissions. It can be seen that five distinct peaks are present in the spectra.

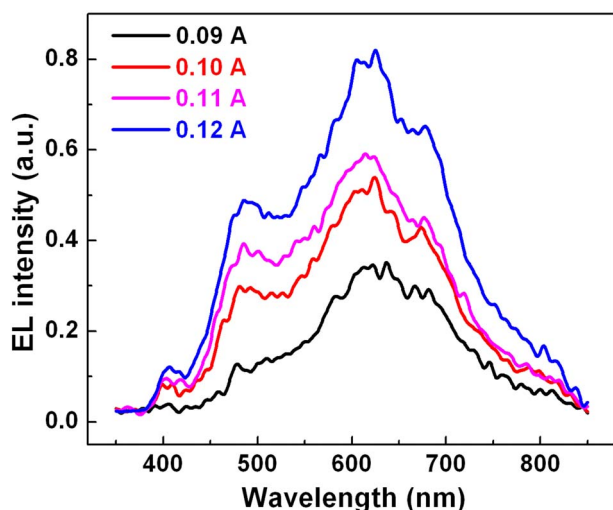


FIG. 4. (Color online) Injection current dependent EL spectra obtained at room temperature.

All the peaks seen in EL spectra are present in the PL spectra nearly around the same wavelength positions. EL and PL spectra being similar confirm that the radiative recombination of the electrons injected from *p*-ZnO and holes from *n*-Si occurs in the ZnO layer.²⁰

In summary, near-band edge emission was observed from the Sb-doped *p*-ZnO/*n*-Si heterojunction diode due to radiative recombination taking place in ZnO. Other emission

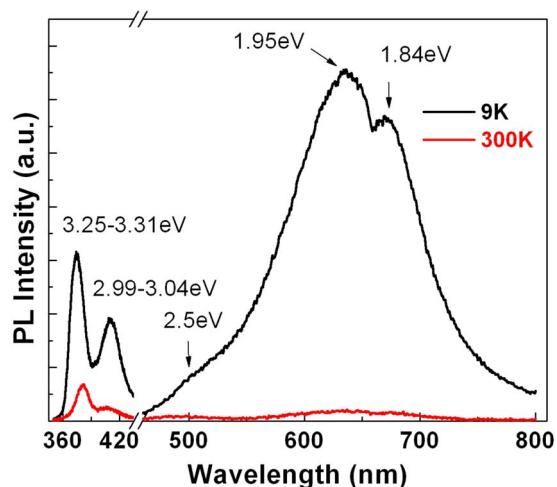


FIG. 5. (Color online) PL spectra from the as-grown sample at 9 K and 300 K.

peaks present in EL spectra originate from the deep levels in ZnO, as seen from the PL evidence. The demonstration of UV emission from Sb-doped *p*-type ZnO films may make Sb-doping of *p*-ZnO promising for LED applications.

This work was supported by the DoD/DMEA through the center for NanoScience and Innovation for Defense (CNID) under the Award No. H94003-06-2-0608 and the UCEI grant. We would like to acknowledge the SIMS measurements performed by Mr. Mikhail Klimov, Materials Characterization Facility, AMPAC, University of Central Florida.

¹U. Ozgur, Ya. I. Alivov, C. Liu, A. Teke, M. A. Reshchikov, S. Dogan, V. Avrutin, S. J. Cho, and H. Morkoc, *J. Appl. Phys.* **98**, 041301 (2005).

²S. J. Pearton, D. P. Norton, K. Ip, and Y. W. Heo, *J. Vac. Sci. Technol. B* **22**, 932 (2004).

³D. C. Look, *Mater. Sci. Eng., B* **80**, 383 (2001).

⁴D. C. Look, B. Claffin, Ya. I. Alimov, and S. J. Park, *Phys. Status Solidi A* **201**, 2203 (2004).

⁵P. Chen, X. Ma, and D. Yang, *J. Appl. Phys.* **101**, 053103 (2007).

⁶Y. Ryu, T. S. Lee, J. Lubguban, H. White, B. J. Kim, Y. S. Park, and C. J. Youn, *Appl. Phys. Lett.* **88**, 241108 (2006).

⁷Z. P. Wei, Y. M. Lu, D. Z. Shen, Z. Z. Zhang, B. Yao, B. H. Li, J. Y. Zhang, D. X. Zhao, X. W. Fan, and Z. K. Tang, *Appl. Phys. Lett.* **90**, 042113 (2007).

⁸A. Tsukazaki, A. Ohtomo, T. Onuma, M. Ohtani, T. Makino, M. Sumiya, K. Ohtani, S. F. Chichibu, S. Fuke, Y. Segawa, H. Ohno, H. Koinuma, and M. Kawasaki, *Nat. Mater.* **4**, 42 (2004).

⁹G. T. Du, W. F. Liu, J. M. Bian, L. Z. Hu, H. W. Liang, X. S. Wang, A. M. Liu, and T. P. Yang, *Appl. Phys. Lett.* **89**, 052113 (2006).

¹⁰J. H. Lim, C. K. Kang, K. K. Kim, I. K. Park, D. K. Hwang, and S. J. Park, *Adv. Mater. (Weinheim, Ger.)* **18**, 2720 (2006).

¹¹J. Bian, W. Liu, J. Sun, and H. Liang, *J. Mater. Process. Technol.* **184**, 451 (2007).

¹²J. C. Sun, J. Z. Zhao, H. W. Liang, J. M. Bian, L. Z. Hu, H. Q. Zhang, X. P. Liang, W. F. Liu, and G. T. Du, *Appl. Phys. Lett.* **90**, 121128 (2007).

¹³W. Liu, S. L. Gu, J. D. Ye, S. M. Zhu, S. M. Liu, X. Zhou, R. Zhang, Y. Shi, Y. D. Zheng, Y. Hang, and C. L. Zhang, *Appl. Phys. Lett.* **88**, 092101 (2006).

¹⁴F. X. Xiu, Z. Yang, L. J. Mandalapu, D. T. Zhao, J. L. Liu, and W. P. Beyermann, *Appl. Phys. Lett.* **87**, 152101 (2005).

¹⁵F. X. Xiu, Z. Yang, L. J. Mandalapu, D. T. Zhao, and J. L. Liu, *Appl. Phys. Lett.* **87**, 252102 (2005).

¹⁶L. J. Mandalapu, F. X. Xiu, Z. Yang, and J. L. Liu, *Appl. Phys. Lett.* **88**, 112108 (2006).

¹⁷L. J. Mandalapu, Z. Yang, F. X. Xiu, and J. L. Liu, *Appl. Phys. Lett.* **88**, 092103 (2006).

¹⁸L. J. Mandalapu, F. X. Xiu, Z. Yang, and J. L. Liu, *J. Appl. Phys.* **102**, 023716 (2007).

¹⁹L. J. Mandalapu, Z. Yang, and J. L. Liu, *Appl. Phys. Lett.* **90**, 252103 (2007).

²⁰A. Tsukazaki, M. Kubota, A. Ohtomo, T. Onuma, K. Ohtani, H. Ohno, S. F. Chichibu, and M. Kawasaki, *Jpn. J. Appl. Phys., Part 2* **44**, L643 (2005).